Macromolecules
ARTICLE

Macromolecules **2009**, *42*, 4257–4261 **4257**
DOI: 10.1021/ma9003727

Micellization Behavior of Poly(*n*-butyl methacrylate)-*block*-poly(2-(acetoacetoxy)ethyl methacrylate)

Reinhard Sigel,[†] Theodora Krasia-Christoforou,[‡] Ines Below, and Helmut Schlaad*

Max Planck Institute of Colloids and Interfaces, Colloid Chemistry, Research Campus Golm, 14424 Potsdam, Germany. [†] Present address: Adolphe Merkle Institute, University of Fribourg, Chemin du Musée 3, Perolles, 1700 Fribourg, Switzerland. [‡] Present address: Department of Mechanical and Manufacturing Engineering, University of Cyprus, P.O. Box 20537, 1678 Nicosia, Cyprus.

Received February 18, 2009; Revised Manuscript Received April 30, 2009

ABSTRACT: A series of poly(*n*-butyl methacrylate)-*block*-poly(2-(acetoacetoxy)ethyl methacrylate)s (PBMA-*b*-PAEMA) were studied according to the formation of core−shell micelles in dilute cyclohexane solution (PBMA → shell, PAEMA → core). Although being a strongly segregating system, the appearance of different shapes of micelles could not appropriately be described by simple space-filling arguments within the geometric model of Antonietti and Förster et al. [*J. Chem. Phys.* **1996**, *104*, 9956−9970]. The model was refined through introduction of the aspect ratio of the core-forming monomer unit for the calculation of geometric packing parameters.

Introduction

Homopolymers and block copolymers based on 2-(acetoacetoxy)ethyl methacrylate (AEMA) are interesting materials in various aspects. First coming into mind is the high affinity of β-dicarbonyl chelates toward metals and metal ions.[1] Polymers of this kind have therefore great application potential in the fields of organic−inorganic hybrid materials[2] and biomineralization processes.[3] Furthermore, β-dicarbonyl compounds are commonly involved in hydrogen-bonding motifs, for example in biological macromolecules (uracil or thymin in nucleic acids)[4] or in synthetic supramolecular assemblies,[5] producing highly ordered superstructures. Accordingly, but nonetheless amazing, a simple PAEMA homopolymer can self-assemble into a complex superstructure like hydrogen-bonded double-helical tube.[6]

Made possible by the progress in block copolymer synthesis,[7,8] we started to investigate the colloidal properties and supramolecular structures of poly(alkyl methacrylate)-*block*-poly(2-(acetoacetoxy)ethyl methacrylate) (here: alkyl = *n*-butyl; PBMA-*b*-PAEMA) in a systematic fashion.[9,10] Especially interesting was the micellization behavior of PBMA-*b*-PAEMA copolymers in dilute cyclohexane solution, cyclohexane being a selective solvent for PBMA. Estimation of the Flory−Huggins interaction parameter from the solubility parameters of BMA and AEMA, which were obtained from group considerations, yielded $\chi \approx 0.8$.[11] This high value of χ indicates that the PBMA and PAEMA segments are highly incompatible and further suggests that block copolymers with a sufficiently high number of repeating units (N) might exhibit a phase behavior which is referred to as the *super strong segregation limit* (SSSL; $\chi N \gg 100$).[12] Accordingly, the micellization behavior of PBMA-*b*-PAEMA should be well described by the geometrical model of strongly segregating block copolymers introduced by Förster and Antonietti.[13,14] However, the model failed to predict the different shapes of PBMA-*b*-PAEMA micelles, which were observed by dynamic and static light scattering (DLS and SLS) and scanning force microscopy (SFM). The aim of the present work is to introduce a refinement of the Förster−Antonietti model for an appropriate description of micellization behavior of PBMA-*b*-PAEMA in dilute cyclohexane solution.

*Corresponding author: Fax ++49-(0)331-567-9502; e-mail schlaad@mpikg.mpg.de.

Experimental Part

Materials. Solvents and chemicals were purchased from Sigma-Aldrich with the highest purity grade available and were used as received. Deuterated solvents (>99.8% D) were purchased from Deutero GmbH (Kastellaun, Germany).

PBMA-*b*-PAEMA copolymers (seven samples) were prepared according to two different procedures described in detail elsewhere.[7,8] The first method[7] involved the azeotropic esterification of PBMA-*b*-PHEMA (HEMA = 2-hydroxyethyl methacrylate), which had been prepared by sequential bibenzoate-catalyzed group transfer polymerization (GTP) of BMA and TMSHEMA (TMS = trimethylsilyl) in tetrahydrofuran (THF) and subsequent acidic hydrolysis of TMS protecting groups, with *tert*-butyl acetoacetate in a benzene−water mixture. The acetoacetylation of hydroxyl groups was virtually quantitative (>95%; ^{1}H NMR) without touching the narrow molecular weight distribution of the starting material (apparent polydispersity index, PDI ∼ 1.1; size exclusion chromatography (SEC)). The PBMA precursors were analyzed by SEC in THF using a PBMA calibration curve to obtain the absolute number-average degree of polymerization of BMA (N_B). The mole fraction of AEMA (f_A) in the copolymer samples was determined by ^{1}H NMR in $CDCl_3$, considering the characteristic signals at δ = 2.27 (AEMA, −C(O)−CH_3) and 3.92 ppm (BMA, −OCH_2−), to calculate the number of AEMA units ($N_A = N_B/(f_A^{-1} - 1)$). The second method[8] employed was the sequential RAFT radical polymerization of AEMA and BMA, producing a block copolymer with a PDI ∼ 1.1. The numbers of repeating units N_A and N_B were determined by ^{1}H NMR end-group analysis in $CDCl_3$. The main characteristics of all samples are summarized in Table 1 (samples **1**, **2**, **4**, **5**, **6**, and **7** were synthesized by GTP/acetoacetylation, sample **3** by RAFT radical polymerization).

Instrumentation and Methods. ^{1}H NMR spectra were recorded at 25 °C on a Bruker DPX-400 spectrometer operating at 400.1 MHz. Signals were referenced to that of traces of nondeuterated solvent arising at δ = 7.24 (chloroform), 1.44 (cyclohexane), or 2.62 ppm (dimethyl sulfoxide, DMSO).

Published on Web 05/21/2009

Table 1. Molecular Characteristics of the PBMA-*b*-PAEMA Diblock Copolymers 1−7 (Synthesized by GTP/Acetoacetylation, 3: RAFT Radical Polymerization) under Investigation[a]

sample	f_A	N_B	N_A	$M_n^{(1)}$ [kg mol^{-1}]	PDI
1	0.07	311	22	48.9	1.26
2	0.10	342	39	57.0	1.05
3	0.13	206	30	35.7	1.10
4	0.14	163	27	28.9	1.15
5	0.15	58	10	9.9	1.07
6	0.22	80	22	16.0	1.03
7	0.45	74	60	23.4	1.09

[a] f_A: mole fraction of AEMA; N_A, N_B: number of AEMA and BMA repeating units, respectively; $M_n^{(1)}$: number-average molecular weight; PDI: polydispersity index), as determined by ^{1}H NMR and SEC.

Size exclusion chromatography (SEC) was performed at 25 °C in THF or chloroform as the eluent at a flow rate of 1.0 mL min^{-1}. Either column set consisted of three MZ-SD*plus* 5 μm columns (10^3, 10^5, 10^6 Å); UV and DRI detectors were employed. Calibration was done with PBMA standards (PSS, Mainz, Germany).

Static light scattering (SLS) experiments were carried out at 20 °C with a frequency-doubled Neodym-YAG laser light source (Coherent DPSS532, intensity 300 mW, λ = 532 nm), an ALV goniometer, and an ALV-5000 multiple-tau digital correlator (ALV GmbH, Langen, Germany). Measurements were performed on 0.1−0.4 wt % (**1**−**6**) or 0.005−0.00625 wt % (**7**) polymer solutions at scattering angles from (15°) 30°−150° at 3° intervals. Data were evaluated by a standard Zimm analysis to provide the molecular weight (M_w) of aggregates, radius of gyration (R_g), and second virial coefficients (A_2). Refractive index increments dn/dc were measured using an NFT-Scanref differential refractometer operating at λ = 633 nm. Dynamic light scattering (DLS) experiments were carried out on a spectrometer consisting of an argon ion laser (λ = 488 nm, 30−600 mW; Coherent Innova 300), a self-constructed goniometer, a single photon detector (ALV SO-SIPD), and a multiple-tau digital correlator (ALV 5000/FAST). DLS autocorrelation functions were measured at different polymer concentrations (see above) and scattering angles (30°, 50°, 70°, and 90°). Measured autocorrelation functions were evaluated with the program FASTORT.EXE.[15] From the obtained diffusion coefficients, hydrodynamic radii (R_h) were calculated using the Stokes−Einstein equation.

Scanning force microscopic (SFM) investigations were performed with a Nanoscope Multimode IIIa (Digital Instruments, Santa Barbara, CA) employing silicon cantilevers (k = 42 N m^{-1}; Olympus Optical Co. Ltd., Japan). Specimens were prepared by spin-coating 0.15 wt % polymer solutions on mica and were scanned in the tapping mode at a resonance frequency of 300 kHz.

Results

Initial SEC and ^{1}H NMR studies suggested that chloroform and tetrahydrofuran (THF) are nonselective solvents for PBMA-*b*-PAEMA; i.e., no aggregation occurred in these solvents. Cyclohexane and dimethyl sulfoxide (DMSO), on the other hand, were found to dissolve selectively one or the other block segment. In cyclohexane, only the NMR signals of PBMA and none of the PAEMA protons could be observed (Figure 1), suggesting the presence of aggregates with a PBMA solvating corona and an insoluble PAEMA core. Aggregates with the inverse structure seem to be formed in DMSO, as only the proton NMR signals of the PAEMA could be detected (spectrum not shown). In the following, we will focus on studies in dilute cyclohexane solution.

Dynamic light scattering (DLS) was applied to investigate the aggregates of PBMA-*b*-PAEMA with respect to their hydrodynamic radius (R_h). Measurements were performed on 0.1−0.4 wt % solutions of the samples **1**−**6** in cyclohexane

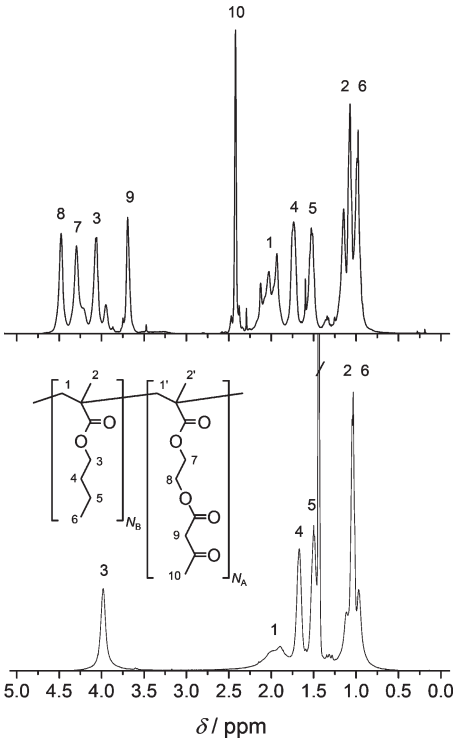

Figure 1. ^{1}H NMR spectra (400.1 MHz) of PBMA-*b*-PAEMA sample **7** in $CDCl_3$ (top) and C_6D_{12} (cyclohexane-d_{12}, / = solvent) (bottom).

Table 2. Experimental Results for Hydrodynamic Radii (R_h), Radii of Gyration (R_g), Aggregation Numbers (Z), and Second Virial Coefficients (A_2) of PBMA-*b*-PAEMA Micelles 1−7 in Dilute Cyclohexane Solution, As Obtained by Light Scattering (DLS and SLS)

sample	R_h [nm]	R_g [nm]	R_g/R_h	Z	$A_2 \times 10^8$ [mol cm^{-3} g^{-2}]	shape of micelles
1	28	22	0.79	101	0.15	spherical
2	32	26	0.81	342	0.15	spherical
3	31	24	0.77	311	0.12	spherical
4	17	n/a	n/a	114	1.00	spherical
5	11	n/a	n/a	93	0.14	spherical
6	12	21	1.75	120	−1.5	spherical/cylindrical
7	49	54	1.10	1025	−81.4	cylindrical

(T = 20 °C). In the case of sample **7**, the sample with the highest mole fraction of AEMA (f_A), the concentration had to be reduced down to 0.005−0.00625 wt % in order to avoid precipitation. Since the glass transition of PAEMA occurs at about +3 °C,[8] the aggregates formed by **1**−**7** in cyclohexane at room temperature were considered to be equilibrium structures.

DLS showed the presence of micellar aggregates with R_h = 11−49 nm (see Table 2). Seemingly, the concentrations of solutions **1**−**7** were chosen to be well above the critical micellization concentration (cmc; not determined). All measured particle size distributions were found to be monomodal, and virtually the same values of R_h were obtained irrespective of scattering angle and concentration. Static light scattering (SLS; see a typical Zimm plot in Figure 2) provided information on the radius of gyration (R_g), the second virial coefficient (A_2), and the weight-averaged molecular weight (M_w) of aggregates of **1**−**7** in cyclohexane. We assume no fractionation effects in the micelles, so the sum of the molecular weights $M^{(1),i}$ of unimers forming an individual micelle of molecular weight M can be expressed by the number-averaged molecular weight $M_n^{(1)}$ of the unimers, $M = \sum_{i=1}^{Z} M^{(1),i} = ZM_n^{(1)}$. The weight-averaged aggregation number thus results as $Z = M/M_n^{(1)}$. Data are summarized in Table 2. Aggregates of **1**−**6** ($f_A \leq 0.22$) are spherical micelles, and those of **7** (f_A = 0.45) are cylindrical micelles, as evidenced by

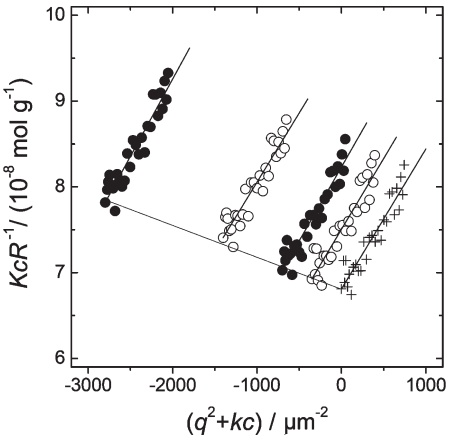

Figure 2. Zimm plot obtained for 0.1−0.4 wt % micellar solutions of PBMA-*b*-PAEMA sample **3** in cyclohexane (T = 20 °C).

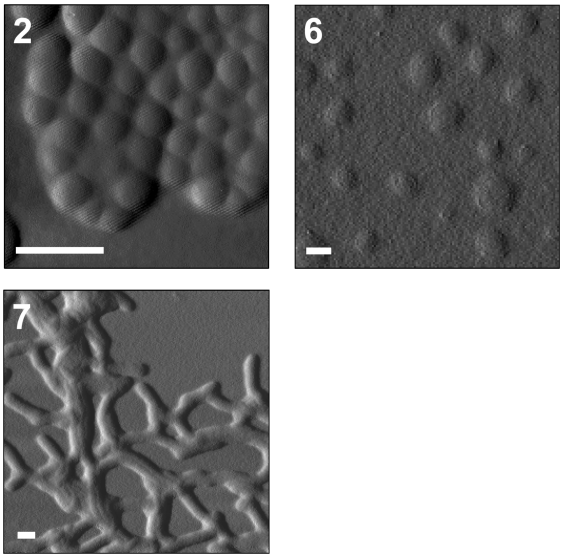

Figure 3. SFM amplitude images of the micellar aggregates of **2**, **6**, and **7**, spin-coated from cyclohexane solution on mica. Scale bars = 100 nm.

SFM (see images in Figure 3). The structure is confirmed by the characteristic values of R_g/R_h for most samples. For **6**, the negative value of A_2 and $R_g/R_h > 1$ indicate that the solution morphology of these micelles deviate from a spherical shape. In fact, in the analysis presented in the discussion section, **6** turns out to be right at the transition between spherical and wormlike micelles. The length of cylindrical micelles **7** could be determined from a Holtzer plot to be ~240 nm.

Discussion

Regarding the high value of the Flory−Huggins interaction parameter χ, it appears adequate to discuss the micellization behavior of PBMA-*b*-PAEMA copolymers in the framework of a model introduced by Antonietti and Förster.[13,14] This model, which is based on a theoretical work of Zhulina and Birshtein,[16,17] describes spherical micelles in the strong segregation limit. Here, the strong enthalpic repulsion of the two blocks of A and B monomers leads to a narrow interface between a nearly pure core composed of the insoluble blocks A and the corona formed by the soluble blocks B. Because of the sharp boundaries, the size of the spherical core is determined by space-filling arguments leading to a scaling relation $Z \propto N_A^2$ of the aggregation number Z with the number N_A of monomers in block A. It is noteworthy that a nonspherical morphology or a weak segregation would

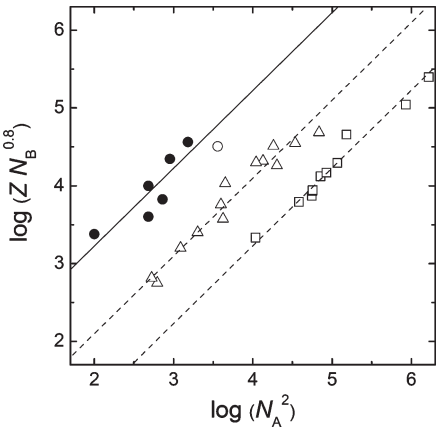

Figure 4. Plot of the aggregation number of block copolymer micelles (Z) as a function of the number of repeating units of the soluble block ($N_B^{0.8}$) and the insoluble block (N_A^2) (according to eq 1):[13] circles: PBMA-*b*-PAEMA/cyclohexane (this work; samples **1**−**6** (closed) and **7** (open)); triangles: PS-*b*-P4 VP/toluene;[13] squares: PS-*b*-PMAA/dioxane−water 80:20 (v/v).[18]

give an exponent of less than 2. The corona on the other hand side is considered as tethered chains, and the area b^2 per chain depends just weakly on the number N_B of monomers in block B. The scaling relation

$$Z = Z_0 N_A{}^{\alpha=2} N_B{}^{\beta=-0.8} \quad (1)$$

has experimentally been confirmed for several block copolymers and low molecular weight surfactants.[13] Figure 4 shows the scaling plot for the spherical micelles **1**−**6** in cyclohexane and, for comparison, for the spherical micelles of polystyrene-*block*-poly(4-vinylpyridine) (PS-*b*-P4VP) in toluene (triangles) and polystyrene-*block*-poly(methacrylic acid) (PS-*b*-PMAA) in dioxane−water 80:20 (v/v) (squares). It can be seen that the aggregation numbers of PBMA-*b*-PAEMA micelles follow the scaling behavior given in eq 1 with $Z_0 = 16.6 \pm 1.2$ but are substantially larger than in the other two micellar systems. Surprisingly, however, the same scaling law seems to hold true for the cylindrical micelles **7** (open circle in Figure 4).

From simple geometric considerations, the volume and interface area of a spherical PAEMA core with a radius R_c are given as

$$(4/3)\pi R_c{}^3 = Z N_A \nu_A \quad (2)$$

$$4\pi R_c{}^2 = Z b^2 \quad (3)$$

$\nu_A = M_A/(\rho_A N_L)$ is the molar volume of an AEMA monomer unit (M_A = 214.22 g mol^{-1}: molar mass of AEMA, ρ_A: specific density of the PAEMA core, N_L: Avogadro's number). Specific densities are accessible from refractive index increment measurements (see Appendix). b^2 denotes the area of a polymer chain at the core−corona interface, and b is the interchain distance. Values of R_c and b, which were obtained for **1**−**6**, are summarized in Table 3.

From eqs 2 and 3, the aggregation numbers are calculated by

$$Z = 36\pi N_A{}^2 \nu_A{}^2 b^{-6} \quad (4)$$

According to results of Förster et al.,[13] the interchain distance b is determined by the number of repeating units of the soluble block (N_B):

$$b = b_0 N_B{}^{\varepsilon} \quad (5)$$

Table 3. Characteristics of the PAEMA Core of PBMA-*b*-PAEMA Spherical Micelles 1−6[a]

sample	V_c [nm^3]	R_c [nm]	b^2 [nm^2]	b [nm]	Δ
1	613	5.3	3.5	1.9	0.11
2	3650	9.6	3.4	1.8	0.11
3	2613	8.5	2.9	1.7	0.13
4	862	5.9	3.8	1.9	0.14
5	280	4.1	2.3	1.5	0.18
6	739	5.6	3.3	1.8	0.16

[a] $V_c = ZN_A\nu_A$: volume, R_c: radius, b^2: area per polymer chain at the core−corona interface, b: interchain distance, Δ: geometric packing parameter (eq 7; $\Delta_0 = 0.53$, $\varepsilon = 2/15$).

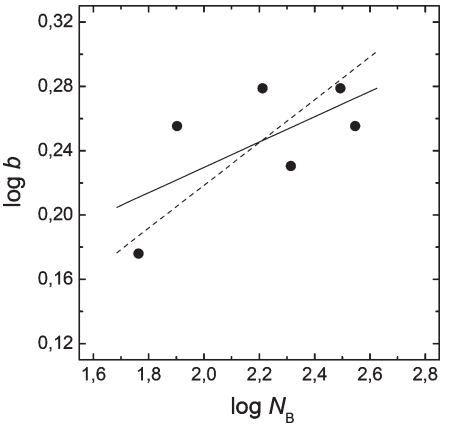

Figure 5. Plot of the interchain distance (b) vs the number of repeating units of the soluble block (N_B). Linear regression of data points yields $\varepsilon = 0.08 \pm 0.05$ as the slope of solid line; the dashed line has a slope of the theoretical value $\varepsilon = 2/15$.

For samples **1**−**6**, it was found $b_0 = 1.6 \pm 0.1$ nm and $\varepsilon = 0.08 \pm 0.05$ (see the corresponding bilogarithmic plot in Figure 5). The value of b_0 is reasonable for block copolymers,[13] but that of ε appears to be too low (theory demands $\varepsilon = \beta/6 = 2/15 \approx 0.13$)[16,17] and is also afflicted with a large experimental error. As will be seen below, the prediction of packing parameters and shapes of aggregates (eq 7) relies very much on the value of ε—we will therefore continue the discussion using the theoretical value of 2/15.

The Z_0 parameter (eq 1) can be written as

$$Z_0 = 36\pi\nu_A{}^2 b_0{}^{-6} = 36\pi\Delta_0{}^3 \quad (6)$$

with $\Delta_0 \equiv \nu_A{}^{2/3} b_0{}^{-2} = 0.53 \pm 0.03$ as a dimensionless intrinsic packing parameter. Δ_0 is related to the geometric packing parameter Δ introduced by Israelachvili[19] through

$$\Delta \equiv \nu(al)^{-1} = (N_A\nu_A)(b^2 N_A \nu_A{}^{1/3})^{-1} = \nu_A{}^{2/3} b^{-2} = \Delta_0 N_B{}^{-2\varepsilon} \quad (7)$$

For surfactants, $\nu/(al)$ is calculated from the optimal headgroup area a, the volume ν, and the contour length l of the hydrocarbon chain. For block copolymers, it is considered $\nu = N_A\nu_A$, $a = b^2$, and $l = N_A\nu_A{}^{1/3}$.[13]

Knowing the value of Δ makes it possible to predict the shape and size of a surfactant or block copolymer micelle. Depending on Δ, they will form spherical micelles ($\Delta < 1/3$), nonspherical or cylindrical micelles ($1/3 \le \Delta \le 1/2$), bilayers or vesicles ($1/2 \le \Delta \le 1$). Equation 7 describes the scaling of Δ with N_B. Only if a block copolymer system exhibits a high enough Δ_0 above 1/3, a transition of the micellar shape can be achieved upon variation of N_B. Table 4 lists the results for Z_0 and the resulting Δ_0 (via eq 6) for the block polymer systems displayed in Figure 4. Among these samples, only PBMA-*b*-PAEMA can show a shape transition

Table 4. Scaling Prefactor Z_0 and the Resulting Intrinsic Packing Parameter Δ_0 for the Three Block Copolymer Systems Displayed in Figure 4

block copolymer system	Z_0	Δ_0
PBMA-*b*-PAEMA/cyclohexane	16.6	0.53
PS-*b*-P4 VP/toluene	1.3	0.23
PS-*b*-PMAA/dioxane−water 80:20 (v/v)	0.17	0.11

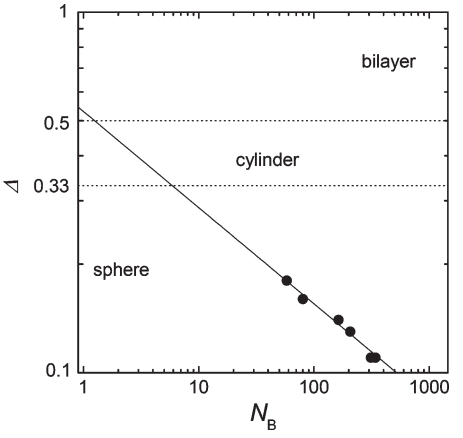

Figure 6. Plot of the geometric packing parameter (Δ) vs the number of repeating units of the soluble block (N_B) for PBMA-*b*-PAEMA micelles **1**−**6** in cyclohexane; the line was calculated according to eq 7 using $\Delta_0 = 0.53$ and $\varepsilon = 2/15$.

within the strong segregation limit. From a molecular point of view, the bulky side chain of the insoluble PAEMA (see Figure 1) results in a high molar volume ν_A with no effect on the core radius R_c, while the side chain of the soluble PBMA is less bulky and therefore b^2 is low. The result is a high value of Δ_0.

For **1**−**6**, it was obtained $\Delta = 0.11$−0.18 (see Table 3), and micelles should therefore all have a spherical shape; this finding is consistent with results from DLS/SLS and SFM measurements. As predicted by eq 7 using $\Delta_0 = 0.53$ and $\varepsilon = 2/15$, the transition from spheres to cylinders should happen when $N_B = 6$ (see the solid line in the bilogarithmic plot of Δ vs log N_B in Figure 6). Cylinders should be formed if $1 < N_B < 6$ and bilayers or vesicles if $N_B = 1$. The existence of cylindrical micelles formed by **7** with $N_B = 74$, clearly seen in the SFM image in Figure 3, is thus not supported by the Antonietti−Förster model.

For the sake of simplicity, Antonietti and Förster calculated the packing parameter Δ employing $l = N_A\nu_A{}^{1/3}$ as the length of the core-forming block segment (cf. eq 7); i.e., monomer units were considered to have a cubical shape, which is certainly not true for AEMA. For local packing issues, however, it is indispensable to distinguish between long monomers with a small side group and short monomers with a large side group. The aspect ratio, which is the ratio of segment lengths parallel and perpendicular to the chain axis, appears to be a suitable parameter for describing the geometry of a given monomer unit. It can be expressed as

$$\sigma^{1/3} = L\nu_A{}^{-1/3} \quad (8)$$

with $L = l_c/N_A = 2.6$ Å as the contour length of the (*all-trans*) AEMA unit. Equation 7 then transforms into

$$\Delta = (N_A\nu_A)(b^2 N_A L)^{-1} = (\nu_A{}^{2/3} b^{-2})(\nu_A{}^{1/3} L^{-1}) = (\nu_A{}^{2/3} b^{-2})\sigma^{-1/3} = \sigma^{-1/3}\Delta_0 N_B{}^{-2\varepsilon} \quad (9)$$

As can be seen from the plots in Figure 7, the aspect ratio of the insoluble monomer has considerable impact on the "phase diagram" of block copolymer micelles; the smaller the value of

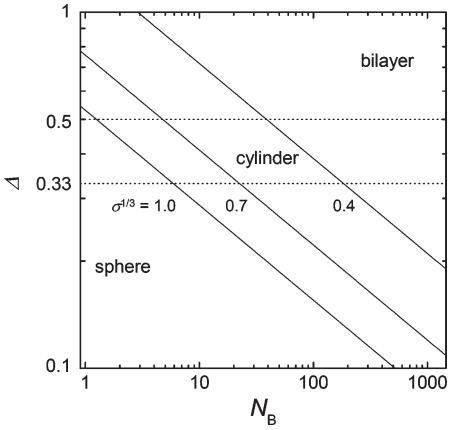

Figure 7. Plot of the geometric packing parameter (Δ) vs the number of repeating units of the soluble block (N_B) for different aspect ratios ($\sigma^{1/3}$) of the insoluble monomer; lines were calculated according to eq 9 using $\Delta_0 = 0.53$ and $\varepsilon = 2/15$.

$\sigma^{1/3}$, the more the shape transition points are shifted to higher N_B. The transition from spheres to cylinders between $N_B = 80$ (**6**, spherical micelles) and 74 (**7**, cylindrical micelles) would be predicted for $\sigma^{1/3} \approx 0.5$; the calculated aspect ratio of AEMA is $\sigma^{1/3} = 0.4$ (eq 8). Hence, within experimental errors, this refined Antonietti−Förster model (eq 9) can quantitatively handle the shape transition observed for PBMA-*b*-PAEMA aggregates. It should be generally applicable to any strongly segregating block copolymer system in a selective solvent.

Conclusion

Poly(*n*-butyl methacrylate)-*block*-poly(2-(acetoacetoxy)ethyl methacrylate) (PBMA-*b*-PAEMA) was found to aggregate into spherical or cylindrical micelles, depending on composition, in dilute cyclohexane solution. Although being a strongly segregating system, the appearance of the different shapes of micelles could not appropriately be described by simple space-filling arguments as proposed by the Antonietti−Förster model. Refinement of this model involved consideration of the aspect ratio of the core-forming monomer unit (here: AEMA) for the calculation of packing parameters. For strong segregation, bulky side chains in the insoluble block (here: AEMA) and the absence of bulky side chains in the soluble block (here: PBMA) are the key concept to design a block copolymer system which shows shape transitions upon a variation of the soluble block length.

Acknowledgment. Birgit Schonert, Andreas Erbe, Olaf Niemeyer, Marlies Gräwert, Rémi Soula, Markus Antonietti, and Erich C. are gratefully thanked for their contributions to this work. Financial support was given by the Max-Planck-Gesellschaft (MPG) and Deutscher Akademischer Austauschdienst (DAAD).

Appendix

Determination of the Density of the Core of Micelles from Refractive Index Increment Data. The refractive index n of a dispersion of particles A with refractive index n_A and density ρ_A in a solvent of refractive index n_0 is the volume average

$$n = n_0 + (n_A - n_0)m_A/(\rho_A V) \qquad \text{(A-1)}$$

of the refractive indices of the constituents, where V is the total volume and m_A is the mass of the particles A. Since $c_A = m_A/V$ is the concentration of A, a comparison with the definition of the refractive index increment $n = n_0 + c_A (dn/dc)_A$ directly gives

$$\rho_A = (n_A - n_0)/(dn/dc)_A \qquad \text{(A-2)}$$

Table 5. Measured Refractive Index Increments (dn/dc) for PBMA-*b*-PAEMA Micelles 1−7 in Cyclohexane and Calculated Refractive Index Increments ($(dn/dc)_A$) and Densities (ρ_A) of the PAEMA Core

sample	dn/dc [cm^3 g^{-1}]	$(dn/dc)_A$ [cm^3 g^{-1}]	ρ_A [g cm^{-3}]
1	0.0545	0.053	1.29
2	0.0582	0.079	1.30
3	0.0553	0.058	1.29
4	0.0534	0.048	1.27
5	0.0472	0.019	1.18
6	0.0531	0.049	1.27
7	0.0690	0.081	1.34

The missing refractive index

$$n_A^2 = (M_A/\rho_A + 2R_M)/(M_A/\rho_A - R_M) \qquad \text{(A-3)}$$

is determined from ρ_A and the molecular weight M_A, where the molar refraction R_M is calculated by summing up tabulated values for the individual chemical groups constituting the polymer.[20] The value for AEMA is $R_M = 48.36N_A$ cm^3 mol^{-1}, where N_A is the number of monomers in a polymer chain. Inserting (A-3) in (A-2) results in an implicit equation for ρ_A. This equation is equivalent to the root of a third-order polynomial which was determined numerically. The refractive index increment of the bare core $(dn/dc)_A$ is calculated from the total index increment

$$dn/dc = w_A(dn/dc)_A + w_B(dn/dc)_B \qquad \text{(A-4)}$$

and the index increment $(dn/dc)_B$ of the shell polymer B, where w_A and w_B are the weight fractions of A and B in the polymer. A measurement of PBMA in cyclohexane gave $(dn/dc)_B = 0.0546$ cm^3 g^{-1}. Results for PBMA-*b*-PAEMA samples **1**−**7** are summarized in Table 5.

References and Notes

(1) Mehrotra, R. C.; Bohra, B.; Gaur, D. P. *Metal β-Diketonates and Allied Derivatives*; Academic Press: New York, 1978.
(2) Kaliyappan, T.; Kannan, P. *Prog. Polym. Sci.* **2000**, *25*, 343–370.
(3) Cölfen, H. *Macromol. Rapid Commun.* **2001**, *22*, 219–252.
(4) Jeffrey, G. A.; Saenger, W. *Hydrogen Bonding in Biological Structures*; Springer: Berlin, 1994.
(5) Lehn, J.-M. *Supramolecular Chemistry - Concepts and Perspectives*; VCH: Weinheim, 1995.
(6) Schlaad, H.; Krasia, T.; Antonietti, M. *J. Am. Chem. Soc.* **2004**, *126*, 11307–11310.
(7) Schlaad, H.; Krasia, T.; Patrickios, C. S. *Macromolecules* **2001**, *34*, 7585–7588.
(8) Krasia, T.; Soula, R.; Börner, H. G.; Schlaad, H. *Chem. Commun.* **2003**, 538–539.
(9) Krasia, T.; Schlaad, H. *ACS Symp. Ser.* **2006**, *928*, 157–167.
(10) Demetriou, M.; Krasia-Christoforou, T. *J. Polym. Sci., Part A: Polym. Chem.* **2008**, *46*, 5442–5451.
(11) Orwoll, R. A. In *Polymer Handbook*, 3rd ed.; Brandrup, J., Immergut, E. H., Eds.; Wiley-Interscience: New York, 1989.
(12) Nyrkova, I. A.; Khokhlov, A. R.; Doi, M. *Macromolecules* **1993**, *26*, 3601–3610.
(13) Förster, S.; Zisenis, M.; Wenz, E.; Antonietti, M. *J. Chem. Phys.* **1996**, *104*, 9956–9970.
(14) Antonietti, M.; Heinz, S.; Schmidt, M.; Rosenauer, C. *Macromolecules* **1994**, *27*, 3276–3281.
(15) Schnablegger, H.; Glatter, O. *Appl. Opt.* **1991**, *30*, 4889–4896.
(16) Zhulina, Y. B.; Birshtein, T. M. *Vysokomol. Soyed.* **1985**, *A27*, 511–517.
(17) Birshtein, T. M.; Zhulina, E. B. *Polymer* **1989**, *30*, 170–177.
(18) Qin, A.; Tian, M.; Ramireddy, C.; Webber, S. E.; Munk, P. *Macromolecules* **1994**, *27*, 120–126.
(19) Israelachvili, J. N. *Intermolecular and Surface Forces*; Academic Press: London, 1985.
(20) Atkins, P. W. *Physikalische Chemie*; VCH: Weinheim, 1987; pp 596 + 872.